

An Exploratory Analysis of Experimental Polar Tensor Data

B. B. Neto,[†] M. M. C. Ferreira, I. S. Scarminio, and R. E. Bruns*

Instituto de Química, Unicamp, C.P. 6154, 13083 Campinas, SP, Brasil (Received: October 16, 1987)

An exploratory statistical study of 157 atomic polar tensors (APT's) taken from 50 molecules is reported. Correlations for all five APT invariants show that comparisons of APT's for different molecules can be made by using mean dipole moment derivative and anisotropy values with only a small loss of statistical information. The use of these values for comparisons with molecular structural parameter values is illustrated. The mean dipole moment derivative values correlate well with electronegativity values for various subgroups of the APT's studied. Anisotropy values can be related to the electronic environment of atoms and bonds adjacent to the atom being studied. Atoms with a polarizable lone pair or an unsaturated bond provoke larger anisotropy values for their neighboring atoms than do completely saturated atoms or bonds. The mean dipole derivative and anisotropy values provide some class discrimination that can be useful for polar tensor transference procedures.

I. Introduction

In the 12 years or so that have elapsed since the publication of the polar tensor formalism in conventional spectroscopic notation,¹ a fairly large number of atomic polar tensors have been obtained from experimental vibrational intensities. Other parametric schemes have been forwarded, based on electrooptical parameters² or charges and charge fluxes,³ but they are ultimately related to the polar tensor formalism and usually require a larger number of parameters. By contrast, the relatively small number of parameters involved in the polar tensor formalism, together with its comparative simplicity, makes it a choice method for the analysis of infrared intensity data.

Much effort has been devoted, within each formalism, to find relations between parameters derived from vibrational intensities and other, more traditional, chemical parameters. Good correlations have been obtained with electronegativities,⁴ force constants,⁵ bond lengths,⁵ degrees of acidity,⁶ percent of ionic character,⁷ and the ability to form molecular complexes.⁶ In all such studies, however, only relatively small groups of molecules were considered, and the conclusions reached were therefore somewhat limited in scope.

In this paper we report a study of a much larger group of molecules. A very extensive set of experimental atomic polar tensors (APT's) is subjected to an exploratory analysis, with a 2-fold objective. In the first place we wish to investigate the possible existence, in this large collection of data, of statistical relations involving the rotationally invariant quantities of the atomic polar tensors. We have chosen the invariants because, unlike the APT elements, they are independent of the orientation of the Cartesian coordinate system for a given molecule and are therefore appropriate for comparisons of data taken from many different sources.

Our second objective is to identify general patterns that will help to define classes or groups of molecules that may act as a guide to the direct transference of atomic polar tensors from one molecule to another. These patterns should also be useful in the construction of similarity models for a more accurate transference of vibrational parameters.⁸ We also expect that a systematic study involving such a large number of APT invariants will lead to a clearer understanding of the relationships between intensity data and molecular structural parameters.

II. The Atomic Polar Tensor Data Set

We gathered a total of 157 atomic polar tensors, for the 50 molecules shown in Figure 1, which also indicates the references containing the original values. For several atoms more than one tensor has been included, reflecting either different experimental intensities or some uncertainty in the reduction of raw data to polar tensor values.

All polar tensors were obtained from experimental gas-phase intensities, but the values of the polar tensor elements depend on

- (1) Person, W. B.; Newton, J. H. *J. Chem. Phys.* **1974**, *61*, 1040.
- (2) Gribov, L. A. *Intensity Theory for Infrared Spectra of Polyatomic Molecules*; Consultants Bureau: New York, 1964.
- (3) Decius, J. C. *J. Mol. Spectrosc.* **1975**, *57*, 348.
- (4) Newton, J. H.; Person, W. B. *J. Chem. Phys.* **1976**, *64*, 3036.
- (5) Gussoni, M.; Jona, P.; Zerbi, G. *J. Chem. Phys.* **1983**, *73*, 6802.
- (6) Gussoni, M.; Castiglioni, C.; Zerbi, G. *J. Chem. Phys.* **1984**, *80*, 1377.
- (7) Bruns, R. E.; Brown, R. E. *J. Chem. Phys.* **1978**, *68*, 880. Kim, K.; King, W. T. *J. Chem. Phys.* **1984**, *80*, 983.
- (8) An application of similarity models is found in Neto, B. B.; Ramos, M. N.; Bruns, R. E. *J. Chem. Phys.* **1986**, *85*, 4515.
- (9) Kondo, S.; Saeki, S. *J. Chem. Phys.* **1982**, *76*, 809.
- (10) van Straten, A. J.; Smit, W. M. A. *J. Chem. Phys.* **1977**, *67*, 970.
- (11) Koga, Y.; Kondo, S.; Saeki, S.; Person, W. B. *J. Phys. Chem.* **1984**, *88*, 3152.
- (12) Kim, K.; King, W. T. *J. Chem. Phys.* **1984**, *80*, 978.
- (13) Kondo, S.; Saeki, S. *J. Chem. Phys.* **1981**, *74*, 6603.
- (14) Newton, J. H.; Levine, R. A.; Person, W. B. *J. Chem. Phys.* **1977**, *67*, 3282.
- (15) Kim, K.; King, W. T. *J. Chem. Phys.* **1979**, *71*, 1967.
- (16) Castiglioni, C.; Gussoni, M.; Zerbi, G. *J. Chem. Phys.* **1985**, *82*, 3534.
- (17) Polavarapu, P. L.; Hess, B. H., Jr.; Schaad, L. J. *J. Mol. Spectrosc.* **1985**, *109*, 22.
- (18) Rogers, J. D.; Hillman, J. J. *J. Chem. Phys.* **1981**, *75*, 1085.
- (19) Kim, K.; King, W. T. *J. Chem. Phys.* **1984**, *80*, 974.
- (20) Ramos, M. N.; Neto, B. B.; Bruns, R. E.; Herrera, O. M. *J. Mol. Struct.* **1986**, *142*, 209.
- (21) Kagel, R. O.; Powell, D. L.; Overend, J.; Ramos, M. N.; Bassi, A. B. M. S.; Bruns, R. E. *J. Chem. Phys.* **1983**, *78*, 7029.
- (22) Neto, B. B.; Bruns, R. E. *J. Chem. Phys.* **1978**, *68*, 5451.
- (23) Bruns, R. E.; Bassi, A. B. M. S. *J. Chem. Phys.* **1976**, *64*, 3053.
- (24) Bruns, R. E.; Bassi, A. B. M. S. *J. Chem. Phys.* **1978**, *68*, 5448.
- (25) Bassi, A. B. M. S.; Bruns, R. E. *J. Phys. Chem.* **1976**, *80*, 2768.
- (26) Kondo, S.; Nakanaga, T.; Saeki, S. *J. Chem. Phys.* **1980**, *73*, 5409.
- (27) Lazzeretti, P.; Zanasi, R. *J. Chem. Phys.* **1986**, *84*, 3916.
- (28) Levin, I. W.; Pearce, R. A. R. *J. Chem. Phys.* **1978**, *69*, 2196.
- (29) Bode, J. H.; Smit, W. M. A.; Visser, T.; Verkruijse, H. D. *J. Chem. Phys.* **1980**, *72*, 6560.
- (30) Jona, P.; Gussoni, M.; Zerbi, G. *J. Phys. Chem.* **1981**, *85*, 2210.
- (31) Nakanaga, T.; Kondo, S.; Saeki, S. *J. Chem. Phys.* **1979**, *70*, 2471.
- (32) Koga, Y.; Kondo, S.; Nakanaga, T.; Saeki, S. *J. Chem. Phys.* **1979**, *71*, 2404.
- (33) Calculated from the intensities given by Kooops, Th.; Visser, T.; Smit, W. M. A. *J. Mol. Struct.* **1985**, *125*, 179.
- (34) Kim, K.; King, W. T. *J. Mol. Struct.* **1979**, *57*, 201.
- (35) Bassi, A. B. M. S.; Bruns, R. E. *J. Chem. Phys.* **1975**, *62*, 3235.
- (36) Kim, K. *J. Phys. Chem.* **1984**, *88*, 2394.
- (37) Kim, K.; McDowell, R. S.; King, W. T. *J. Chem. Phys.* **1980**, *73*, 36.
- (38) Calculated from the intensities reported in Saeki, S.; Mizuno, M.; Kondo, S. *Spectrochim. Acta, Part A* **1976**, *32A*, 403, assuming both $\partial\bar{\mu}/\partial Q$'s to be negative.
- (39) Kagel, R. O.; Powell, D. L.; Overend, J.; Ramos, M. N.; Bassi, A. B. M. S.; Bruns, R. E. *J. Chem. Phys.* **1982**, *77*, 1099.
- (40) Bassi, A. B. M. S.; Bruns, R. E. *J. Phys. Chem.* **1975**, *79*, 1880.
- (41) Kagel, R. O.; Powell, D. L.; Overend, J.; Hopper, M. J.; Ramos, M. N.; Bassi, A. B. M. S.; Bruns, R. E. *J. Phys. Chem.* **1984**, *88*, 521.

[†] Permanent address: Depto. de Química Fundamental, UFPE, 50000 Recife, PE, Brasil.

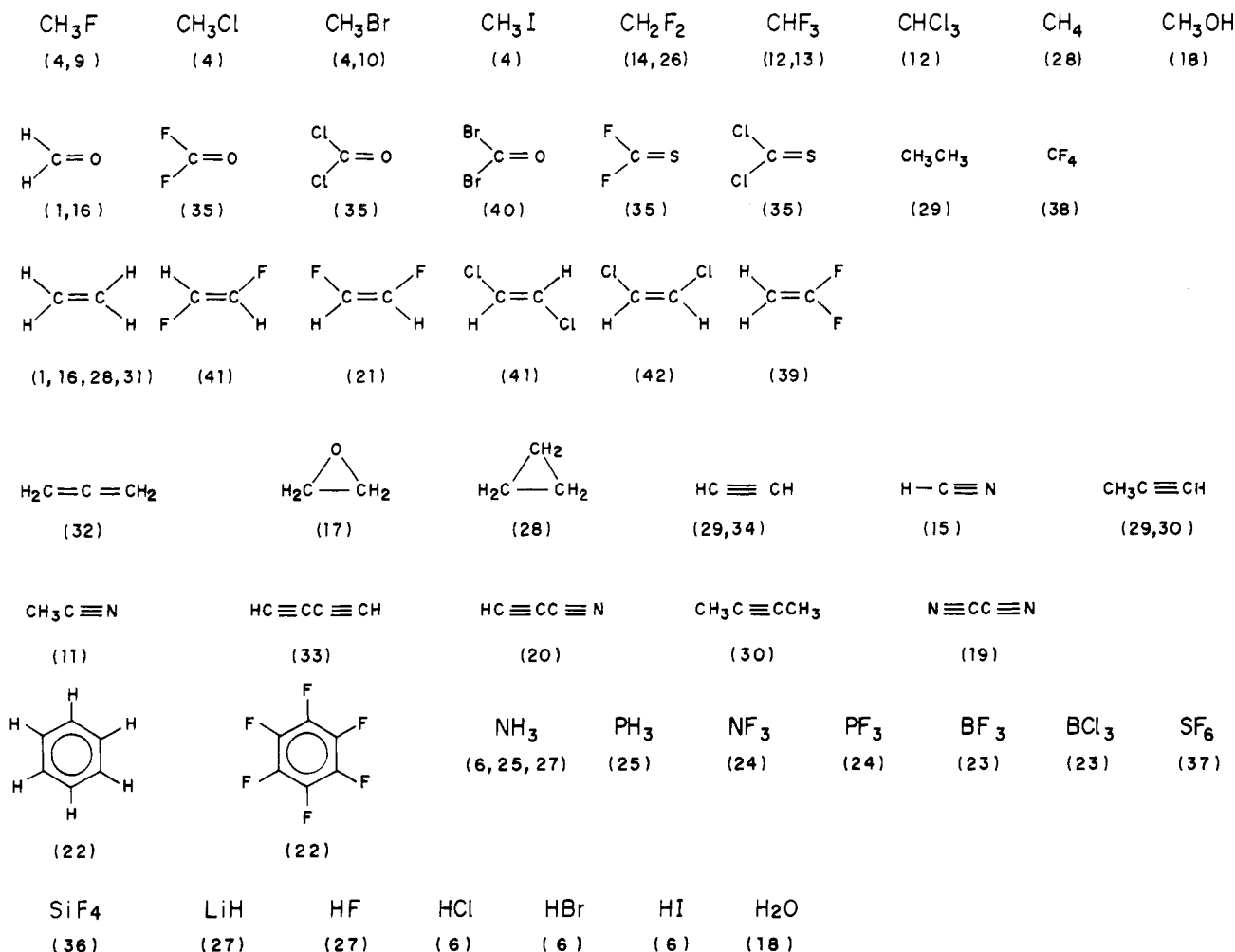


Figure 1. Molecules having experimental polar tensors considered in this work. References are indicated in parentheses.

which algebraic signs are ascribed to the dipole moment derivatives with respect to the normal coordinates of vibration. The determination of these signs usually requires additional information from molecular orbital calculations, from the isotope invariance of certain intensity parameters, or from the nature of Coriolis interactions and therefore can be a source of uncertainty.

An atomic polar tensor (APT) contains the derivatives of the three Cartesian-components of the molecular dipole moment with respect to the three Cartesian displacements of the atom in question. For the 157 APT's studied here only five—at most—of the nine elements have nonzero values, and it is always possible to find an orientation of the Cartesian frame in which the tensor has the form

$$\mathbf{P}_X^{(\alpha)} = \begin{pmatrix} p_{xx} & 0 & p_{xz} \\ 0 & p_{yy} & 0 \\ p_{zx} & 0 & p_{zz} \end{pmatrix} \quad (1)$$

The mean dipole derivative, \bar{p}_α , the atomic effective charge, χ_α , and the anisotropy, β_α^2 , are the invariants commonly appearing in the literature.⁴³ For a given APT their values are unaffected by the orientation of the Cartesian coordinate system.

Two more invariants can be obtained from the secular equation of an APT, which can be written as

$$f(\lambda) = \lambda^3 - (\text{Tr } \mathbf{P}_X)\lambda^2 + C\lambda - D = 0$$

λ standing for the eigenvalues. Since the coefficients of the secular equation are not affected by unitary transformations, $\text{Tr } \mathbf{P}_X$, C ,

and D , are invariant under a rotation of the Cartesian frame. $\text{Tr } \mathbf{P}_X$, the polar tensor's trace, is simply 3 times the mean dipole moment derivative, but C and D are two new invariants. D represents the APT determinant and C is the sum of the minors of the diagonal elements. For the APT of eq 1 we have

$$C = p_{xx}p_{yy} + p_{yy}p_{zz} + p_{xx}p_{zz} - p_{zx}p_{xz} \quad (2)$$

The mathematical relations involving these five invariant quantities for a given tensor are complicated, with the exception of the equation relating the square of the effective charge to the anisotropy and the square of the mean dipole moment derivative⁴³

$$\chi_\alpha^2 = (\bar{p})^2 + (2/9)\beta_\alpha^2 \quad (3)$$

With our large data set statistical studies investigating the relations between the five invariant quantities become feasible. Correlation coefficients, principal component analyses, and bidimensional graphs involving the invariants are useful in discovering statistical redundancies in the APT data and in clarifying the relative advantages and disadvantages of these invariant quantities in polar tensor and intensity studies.

Instead of employing directly the values of β^2 , C , and D we shall use β , $C^{1/2}$, and $D^{1/3}$, to make all invariants have the same unit, namely charge. For β , χ , and $C^{1/2}$, which are defined by quadratic equations, absolute values will always be used.

III. Results and Discussion

The atomic polar tensor data for the molecules in Figure 1 can be represented graphically as points in a five-dimensional space where each coordinate axis corresponds to an invariant quantity. A principal component analysis⁴⁴ in this space showed that 92% of the total data variance is explained by the first two principal

(42) Hopper, M. J.; Overend, J.; Ramos, M. N.; Bassi, A. B. M. S.; Bruns, R. E. *J. Chem. Phys.* **1983**, *79*, 19.

(43) Person, W. B. In *Vibrational Intensities in Infrared and Raman Spectroscopy*; Person, W. B., Zerbi, G., Eds.; Elsevier: Amsterdam, 1982; Chapter 4.

(44) Wold, S.; Sjostrom, M. In *Chemometrics: Theory and Application*; Kowalski, B. R., Ed.; American Chemical Society: New York, 1977.

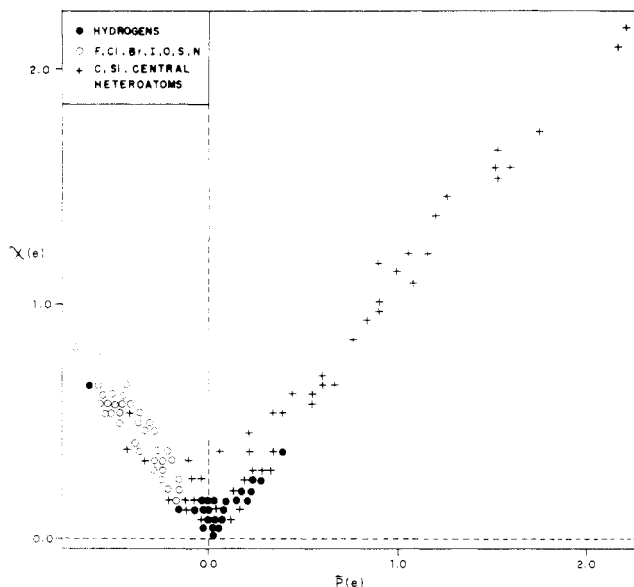


Figure 2. Plot of the effective charge (χ) against the mean dipole derivative (\bar{p}) for all APT's. Several points are left out due to superposition, near the bottom of the plot (atomic units).

components. This means that although the formal dimensionality of the APT invariant data is five, the intrinsic dimensionality is about two.

The number of independent elements in a *molecular* polar tensor is equal to the number of infrared-active fundamental bands,⁴⁵ and the elements are distributed among the APT's corresponding to the nonequivalent atoms in the molecule. Even for molecules of low symmetry with a large number of active fundamentals there will be, on the average, less than three independent elements per APT. As most of the molecules in Figure 1 have reasonably high symmetry, the bidimensional nature revealed by the principal component analysis is not surprising.

The statistical redundancy in the invariant APT data can be characterized with the aid of correlation coefficients. Table I contains the values of the correlation coefficients calculated for all possible pairs of the invariant quantities. Very high correlation coefficients are observed for the $\bar{p}:D^{1/3}$ (0.930) and the $\chi:C^{1/2}$ (0.940) pairs. Two-dimensional graphs (not presented here) for these pairs show very strong linear behaviors, as might be expected from the values of the coefficients, implying that $C^{1/2}$ and $D^{1/3}$, derived from the APT secular equation, contain essentially the same statistical information as the more commonly used invariants, χ and \bar{p} , at least for the molecules studied here. The latter invariants, however, are advantageous because their physical interpretation is straightforward.

Moderate values of the correlation coefficients are found for the $\bar{p}:\chi$ (0.674), $\bar{p}:C^{1/2}$ (0.714), $\chi:D^{1/3}$ (0.650), and $D^{1/3}:C^{1/2}$ (0.705) pairs of variables. Each of these pairs contains either χ or $C^{1/2}$, which have sign ambiguities due to the extraction of the square root. In Figure 2 values of the effective charge, arbitrarily taken as positive in these exploratory calculations, are plotted against values of the mean dipole derivative. Due to overlapping, several points, mostly representing hydrogen APT's, have been left out, near the bottom of the plot.

The graph in Figure 2 contains two distinct linear segments. The right segment shows a large positive correlation between \bar{p} and χ , whereas the left one exhibits a strong negative correlation, implying that the correlation coefficient of 0.674 would be much higher if the signs calculated for the mean dipole derivative were also given to the corresponding effective charge.

This is not an unreasonable suggestion. Most of the hydrogen polar tensors, with the noticeable exception of the ones for the highly ionic molecules LiH and HF, have values close to zero for both \bar{p} and χ . Carbon polar tensors for the hydrocarbons also

TABLE I: Correlation Coefficients for the Five Invariant Quantities of the 157 Atomic Polar Tensors^a

	\bar{p}	χ	β	$D^{1/3}$	$C^{1/2}$
\bar{p}		0.674	0.215	0.930	0.714
χ			0.614	0.650	0.940
β				0.121	0.427
$D^{1/3}$					0.705
$C^{1/2}$					

^a \bar{p} , χ , β , $D^{1/3}$ and $C^{1/2}$ are respectively the mean dipole moment derivative, the effective charge, the square root of the anisotropy, the cubic root of the APT determinant, and the square root of the sum of the minors of the APT diagonal elements.

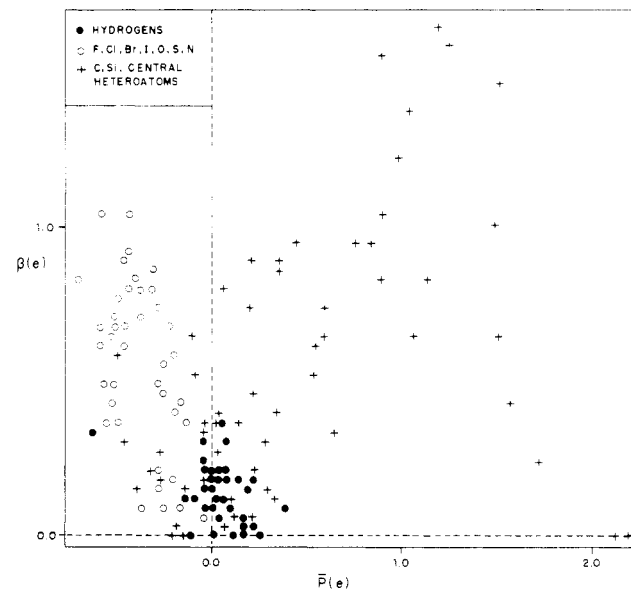


Figure 3. Plot of the square root of the anisotropy (β) against the mean dipole derivative (\bar{p}) for all APT's. Several points are left out due to superposition, near the bottom of the plot (atomic units).

have very small absolute values for these variables, the smallest absolute values of \bar{p} and χ occurring for the carbon APT in methane. The points corresponding to APT's of the more electronegative elements (F, Cl, Br, O, N) are concentrated toward the left, in the region of negative \bar{p} values, whereas the right segment is occupied mostly by the invariants of central atoms (carbons or otherwise) bonded to heteroatoms. It seems, then, that the mean dipole derivative serves as indicator of the electronegative (or electropositive) character of the atom and that the same function could be performed by the effective charge, if the proper algebraic sign were ascribed to it. In other words, the values of \bar{p} and χ contain essentially the same statistical information, with the exception of the sign information, which is lacking for the χ values. The same holds for $C^{1/2}$, since it is highly correlated with χ . The graphs for the other three pairs with moderate correlation coefficient values ($\bar{p}:C^{1/2}$, $\chi:D^{1/3}$ and $D^{1/3}:C^{1/2}$) are quite similar to the graph for the $\bar{p}:\chi$ pair, which we have just discussed.

The lowest correlation coefficients in Table I occur for the pairs of variables containing the anisotropy, $\bar{p}:\beta$ (0.215), $\chi:\beta$ (0.614), $\beta:D^{1/3}$ (0.121), and $\beta:C^{1/2}$ (0.427). In Figure 3 the square root of the anisotropy is plotted against the mean dipole derivative for all APT's. Along the abscissa this graph is of course exactly the same as the one in Figure 2, with the more electronegative atoms situated toward the left and the central atoms bonded to them located toward the right. The low correlation coefficient (0.215), however, is reflected in the considerable scatter of the points.

The use of absolute values for both χ and β leads to a merging of the points representing APT's of terminal electronegative atoms and points representing central carbons and, therefore, to a somewhat spuriously larger correlation coefficient for the $\chi:\beta$ pair of variables. In view of this, and of the small values for the remaining correlation coefficients, we may say that β is not

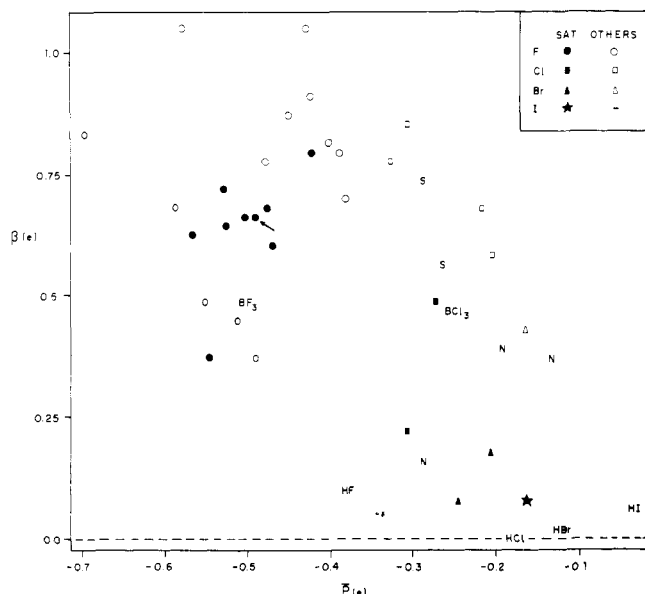


Figure 4. Plot of the square root of the anisotropy (β) against the mean dipole derivative ($\bar{\rho}$) for the APT's of terminal heteroatoms (atomic units).

well-correlated with any of the other variables.

In summary two invariants, $\bar{\rho}$ and β , can be used instead of all five quantities, with only a small loss of statistical information. This conclusion is consistent with the one obtained from the principal component analysis, where of the two principal components explaining 92% of the statistical variance one is essentially the arithmetic mean of $\bar{\rho}$, χ , $C^{1/2}$, and $D^{1/3}$ and the other is dominated by β .

In various polar tensor studies attempts have been made to interpret the effective charge quantity by relating its values with electronegativity values, with Mulliken net charges, or with other parameters. When restricted to groups of similar polar tensors where one can assume all effective charges to have the same sign, this should not lead to problems. However, for comparisons based on more extensive sets of polar tensors, in which the invariability of the sign of the effective charge cannot be ascertained, the use of the mean dipole derivative seems advantageous. Not only is the sign problem automatically taken care of, but the $\bar{\rho}$ values for all atoms in a neutral species add up to zero, making them particularly suitable for comparisons with Mulliken net charges. Accordingly in the following sections, where selected subsets of the APT invariants are studied, our discussion is based on β vs $\bar{\rho}$ graphs.

Terminal Heteroatoms. Figure 4 shows all the APT's comprising this subgroup. The halogens are represented by two kinds of geometrical symbols. The black symbols stand for halogens bonded to saturated atoms, whereas the white ones correspond to halogens bonded to atoms participating in an unsaturated bond or containing a polarizable lone pair. The hydrogen halides and the boron trihalides are indicated by molecular formulas, and the other heteroatoms are represented by their atomic symbols.

The mean dipole derivative values roughly separate the halogens of the polyatomic molecules into groups, with the more negative $\bar{\rho}$ values being associated with the more electronegative halogens. The same pattern, but displaced to the right, is repeated for the hydrogen halides. For the remaining APT's the situation is not so clear-cut. As one might anticipate, the oxygens, which overlap the fluorine class for saturated molecules, stay to the left of the nitrogens. In between, however, lie the two sulfur atoms, mixed with the chlorines.

Figure 4 shows that the β and $\bar{\rho}$ values allow a very good discrimination of the kind of atom to which a halogen is attached. With only one exception all the black symbols, representing halogens bonded to saturated atoms, lie in the bottom left triangle, or close to the diagonal running from the lower right-hand corner to the upper left-hand corner of the graph. The sole exception

TABLE II: Averages and Standard Deviations^a of Mean Dipole Moment Derivatives and Anisotropy Values for Several Classes of Molecules (Atomic Units)

	$\bar{\rho}$	β
F (sat)	-0.506 ± 0.043	0.642 ± 0.117
F (unsat)	-0.442 ± 0.065	0.873 ± 0.098
Cl (sat)	-0.287 ± 0.025	0.354 ± 0.200
Cl (unsat)	-0.263 ± 0.061	0.727 ± 0.119
Br (sat) ^b	-0.224	0.131
Br (unsat)	-0.160	0.260
BF ₃	-0.507	0.485
BCl ₃	-0.247	0.465
H-C	0.009 ± 0.049	0.160 ± 0.042
H-C=	0.020 ± 0.037	0.222 ± 0.042
H-C≡	0.219 ± 0.028	0.023 ± 0.011
C(sp ³)	0.632 ± 0.611	0.419 ± 0.321
C(sp ²)	0.428 ± 0.519	0.855 ± 0.474
C(sp)	-0.076 ± 0.161	0.157 ± 0.140

^a The standard deviations arise from at least two sources, differences in the chemical environments of the atom studied and experimental error. ^b Values for the CH₃Br and Br₂CO molecules.

corresponds to one¹⁴ of the two fluorine polar tensors for methylene fluoride considered in this work. Its presence among the white circles representing fluorines in an unsaturated or lone pair environment suggests that the point corresponding to the alternative, more recent results,²⁶ indicated by an arrow in Figure 4, is to be preferred if similarity with other fluorines in the "saturated" class is taken into account. This may well be the case, considering the extensive overlapping verified in the infrared spectrum of methylene fluoride.^{14,26}

For each type of halogen the anisotropy values are higher for the halogen in an unsaturated or lone pair environment than for that in a totally saturated one. In Table II average and standard deviation values are given for the fluorine and the chlorine APT's in these two situations. Also listed are the fluorine and chlorine $\bar{\rho}$ and β values for BF₃ and BCl₃. These values, like the visual display in Figure 4, favor the classification of the F and Cl APT's of these molecules as belonging to the "saturated environment" class. The classification of the Cl APT for BCl₃ is less clear-cut than the one for its fluorine counterpart. More experimental data would be useful in providing a more secure classification.

The results given in Figure 4 and Table II for the anisotropy values can be explained by a qualitative consideration of the electronic structure of these molecules. Contributions to the APT of a given atom from changes in the electronic structure of neighboring atoms are expected to increase the APT polarizability. These contributions arise from the charge flux and overlap terms in the charge-charge flux overlap (CCFO) model.⁴⁶ Since electrons participating in double bonds and lone pairs are more polarizable, i.e., have lower ionization potentials, than those of a saturated bond, a smaller APT anisotropy is expected for an atom in a completely saturated environment.

Hydrogens. Figure 5 contains a graph of β vs $\bar{\rho}$ for the hydrogen APT's of all molecules in Figure 1, except LiH. The hydrogen in lithium hydride has a mean dipole derivative of $-0.652e$, whereas all other hydrogens have $\bar{\rho}$ values between $-0.119e$ and $0.382e$. Clearly this very negative hydrogen is an outlier for any of the possible classes of the hydrogen APT's.

In Table II averages and standard deviations for $\bar{\rho}$ and β values are presented for hydrogens bonded to carbon atoms with sp³, sp², and sp hybridizations. The hydrogen atoms bonded to sp carbons have much higher $\bar{\rho}$ values and much lower β values than those bonded to sp² and sp³ carbons. The higher $\bar{\rho}$ values correspond to very positively charged (acidic) hydrogens, which are known to be present in the HCN and C₂H₂ molecules. The hydrogen $\bar{\rho}$ values for C₆H₂, HC₃N, and CH₃CCH are very similar to these values for HCN and C₂H₂, as indicated by the small standard

(46) Person, W. B.; Zilles, B.; Rogers, J. D.; Maia, R. G. A. *J. Mol. Struct.* **1982**, *80*, 297.

(47) Person, W. B.; Steele, D. *Molecular Spectroscopy*; Chemical Society: London, 1974; Vol. 2, pp 357-438.

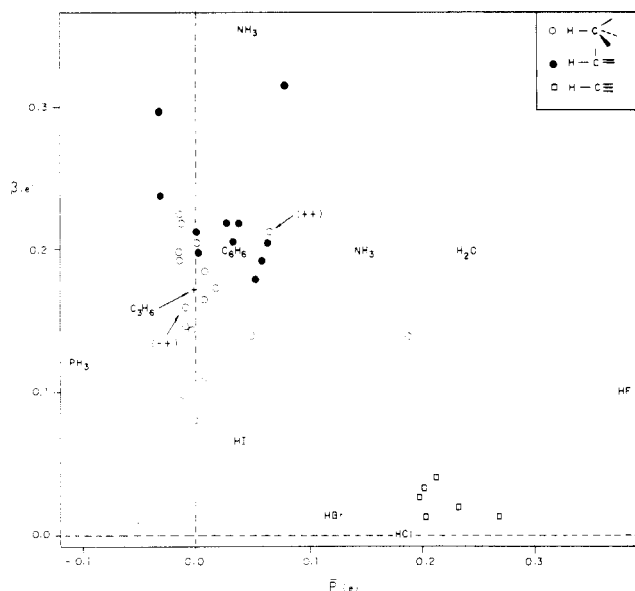


Figure 5. Plot of the square root of the anisotropy (β) against the mean dipole derivative (\bar{p}) for the hydrogen APT's (atomic units).

deviation, $\pm 0.028e$, for the \bar{p} values in this class. The low anisotropy values, on the other hand, are a consequence of the high symmetry of these linear molecules. Although the π electrons in the CC triple bond are very polarizable, the high order symmetry axis forbids nonzero off-diagonal elements and forces two of the diagonal elements to be equal in the acidic hydrogen APT's. Both of these effects of course tend to lower the APT anisotropy.

The polar tensor \bar{p} and β values then allow the hydrogens bonded to sp carbons to be well discriminated from other organic hydrogens. In other words, the former hydrogens form a tight isolated class, in which direct transference of hydrogen APT's should be quite accurate. Indeed, we recently used this class as the basis for a similarity transference of polar tensors.⁸

The classes of hydrogens bonded to sp^2 and sp^3 carbons are considerably superposed, as inspection of Figure 5 and of Table II will confirm. Nevertheless the β values for hydrogens bonded to sp^2 carbons are in general clearly larger than these values for hydrogens bonded to sp^3 carbons, whereas the \bar{p} values occupy nearly the same interval in both classes. This is reminiscent of the similar situation found in the previous section for the halogen APT invariants.

Two of the points in the H-C (sp^3) class belong to different sign choices (indicated in Fig. 5) for the dipole moment derivatives $\partial\bar{p}/\partial Q_6$ and $\partial\bar{p}/\partial Q_7$ in the B_1 symmetry species of methylene fluoride. An analysis of Coriolis interactions²⁶ fixes $\partial\bar{p}/\partial Q_7$ as positive but leaves some doubt as to the sign of $\partial\bar{p}/\partial Q_6$. Since the (++) set leads to a better prediction of the experimental intensities of CH_2F_2 and CD_2F_2 , it is finally preferred in ref 26, but this is reported as extremely surprising, being in disagreement with the so-called "CH stretching criterion"⁴⁴ and with CNDO/2 calculations. Figure 5 shows that the (++) point is located quite far from the region defined by the other, presumably similar, hydrogens bonded to sp^3 -hybridized carbons. The alternative (-+) sign choice, on the other hand, fits well in that region and is therefore favored by similarity considerations. Is the hydrogen in CH_2F_2 really an outlier regarding the other sp^3 -bonded hydrogens, as the position of the (++) point seems to imply? Perhaps, as suggested in ref 26, a good ab initio calculation might be able to provide a definite answer.

Carbon Atoms. The β vs \bar{p} graph for this group is presented in Figure 6. Compared with previous plots, the distribution of the carbons seems rather diffuse and without remarkable discriminatory properties. This should not come as a surprise, given the wide variety of chemical moieties represented in Figure 6. Nevertheless, the \bar{p} values for the carbon APT's roughly increase with the increasing electronegativity of the substituents. This is most noticeable for the halogenated methanes, whose points are

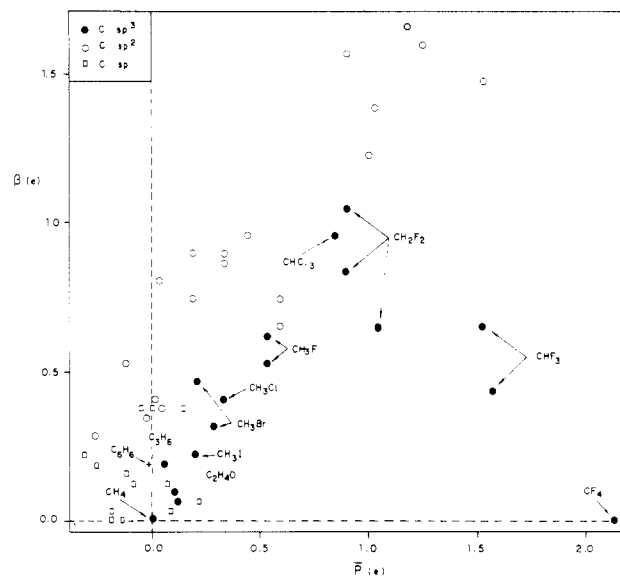


Figure 6. Plot of the square root of the anisotropy (β) against the mean dipole derivative (\bar{p}) for carbon APT's (atomic units).

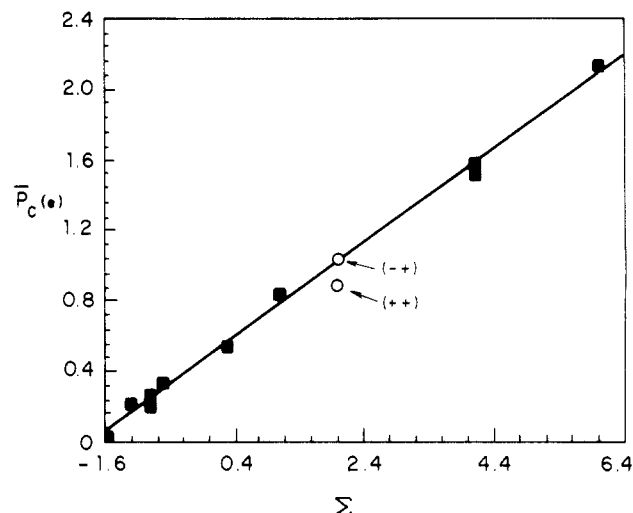


Figure 7. Regression of \bar{p} values (atomic units) of carbon atoms in halogenated methanes on the quantity Σ defined in the text. The signs in parentheses refer to the dipole moment derivatives in block B_1 of CH_2F_2 (see text).

individually identified in the β vs \bar{p} graph. A regression of the carbon \bar{p} values for these molecules on the quantity Σ defined below is shown in Figure 7.

Σ is obtained by subtracting the electronegativity of carbon from the electronegativities of each of the four atoms attached to it and then adding the results. On the Pauling scale the values of Σ range from -1.6 in methane to 6.0 in CF_4 . The conflicting values for the two sign choices in CH_2F_2 were not included in the regression calculation. The fit is strikingly good, with a correlation coefficient of 0.998, the regression equation being

$$\bar{p}_c = 0.486 + 0.267\Sigma$$

The values of \bar{p}_c resulting from the two sign choices for the B_1 dipole moment derivatives in CH_2F_2 are also plotted in Figure 7. The (++) point is situated a little below the regression line, while the alternative (-+) point falls right on it. This lends further support to the idea that the (++) sign choice for the B_1 species of CH_2F_2 is perhaps not the correct one. Moreover, the goodness of fit of the regression line in this case opens the possibility of prediction of \bar{p}_c values for similar molecules in the same class, with obvious implications for the sign choices of the corresponding dipole moment derivatives.

The sp carbons have small negative \bar{p} values, which correlate with the positive \bar{p} values for the hydrogens attached to them. On

the other hand the β values for both these carbon and hydrogen atoms are relatively low, for symmetry reasons. The average anisotropy values in Table II for the carbon classes are ordered as $\beta_{c,sp^2} > \beta_{c,sp^3} > \beta_{c,sp}$, the same ordering observed for their associated hydrogens.

IV. Conclusions

For the extensive set of APT's examined in this work the following conclusions can be made. Comparisons of APT's for different molecules can be made by using $\bar{\rho}$ and β values instead of values for all five tensor invariants with only a small loss of statistical information. Effective charge values are strongly correlated with the absolute values of the mean dipole moment derivatives. The use of $\bar{\rho}$ values for comparisons with molecular structural parameters is suggested since these values contain algebraic sign information. For the Mulliken charge parameters obtained from ab initio molecular orbital calculations the $\bar{\rho}$ in-

variant has the additional advantage of summing to zero for all the atoms in a molecule. However comparisons of effective charge values with more commonly used molecular parameter values can be useful if care is taken to restrict studies to groups of molecules for which sign changes of the effective charge invariant are not expected.

The mean dipole moment derivative values correlate well with electronegativity parameter values for various subsets of the APT set studied here. Differences in the anisotropy values observed for the APT's can be related to the electronic environment of atoms and bonds adjacent to the atom being studied. Larger anisotropy values are encountered for APT's of atoms adjacent to an unsaturated bond or to an atom with a polarizable lone pair than for APT's of atoms in a completely saturated environment. The $\bar{\rho}$ and β values allows some class discrimination for APT's of the same kind of atom which can be useful as a guide for polar tensor transference procedures.

Evidence from Alkali-Metal NMR Spectroscopy for Ion Pairing in Alkaline Silicate Solutions

A. V. McCormick, A. T. Bell,* and C. J. Radke

Center for Advanced Materials, Lawrence Berkeley Laboratory, and Department of Chemical Engineering, University of California, Berkeley, California 94720 (Received: March 4, 1988; In Final Form: July 15, 1988)

Interactions between alkali-metal cations and silicate anions in silicate solutions were investigated by cation NMR spectroscopy. The concentration of cation-anion pairs was determined from the chemical shift and the resonance line widths. The concentration of ion pairs involving large anions increases with increasing cation size. For silicate solutions in which there is a distribution in cation size, the concentration of ion pairs exhibits a maximum with increasing cation size. This maximum is interpreted in terms of the selectivity of ion-pairing reactions.

Introduction

Alkali-metal cations are known to influence the chemistry of silicate anions in alkaline aqueous solution. Information obtained from ^{29}Si NMR, Raman spectroscopy, and trimethylsilylation/chromatography has shown that, for a fixed silica concentration and silicate ratio, the molecular weight of the silicate anions increases with the size of the cation.¹⁻³ Cation size has also been observed to influence the reactivity of silicate anions with aluminate anions⁴⁻⁶ and with this the selectivity of zeolite synthesis.⁷ While the exact means by which cations affect the chemistry of silicate anions is not known, there is increasing evidence that cation-anion pairing plays an important role.^{1,8} Because of this, there is a strong interest in learning more about the pairing between alkali-metal cations and silicate anions.

The chemical environment of alkali-metal cations can be probed by NMR spectroscopy. Each alkali metal has a high abundance of an NMR-active isotope. Interactions of the cations with water

and anionic species are reflected by the chemical shift and the width of the cation line.⁹ This paper describes the use of NMR spectroscopy to characterize the interactions of alkali-metal cations with hydroxide and silicate anions in alkaline solutions. The experimental data provide direct evidence of cation-anion pairing and the effects of silicate anion size on its effectiveness in forming ion pairs.

Experimental Section

Alkali-metal silicate solutions were prepared from Baker analyzed SiO_2 gel, reagent grade alkali-metal hydroxides, and deionized water. Stock solutions at about 3 mol % SiO_2 , $[\text{SiO}_2]/[\text{M}_2\text{O}] = R = 3.0$ ($M = \text{alkali metal}$), were aged in polypropylene bottles for periods of several weeks to assure that all the SiO_2 dissolved. Samples were then formulated with extra water and base to achieve a desired composition and were further aged for several days.

The NMR spectra of ^7Li , ^{23}Na , ^{39}K , ^{87}Rb , and ^{133}Cs were recorded on a Bruker AM-500 spectrometer. Care was taken to utilize sufficiently large spectral widths to avoid foldback of peaks. Chemical shifts were externally referenced to dilute salt solutions, and no field/frequency lock was employed.

Results

Alkali-metal NMR spectra were taken of both silicate and hydroxide solutions at room temperature. Only a single resonance

(1) McCormick, A. V.; Bell, A. T.; Radke, C. J. In *Perspectives in Molecular Sieve Science*; Flank, W. H., Ed.; American Chemical Society: Washington, DC, 1988; ACS Symp. Ser. No. 386, p 222.

(2) Dutta, P. K.; Shieh, D. C. *Zeolites* 1958, 5, 135.

(3) Ray, W. H.; Plaisted, R. J. *J. Am. Chem. Soc.* 1986, 108, 7159.

(4) Durouane, E. G.; Nagy, J. B.; Gabelica, Z.; Blom, N. *Zeolites* 1982, 2, 299.

(5) Dent Glasser, L. S.; Harvey, G. *J. Chem. Soc., Chem. Commun.* 1984, 1250.

(6) Gabelica, Z.; Blom, N.; Derouane, E. G. *Appl. Catal.* 1983, 5, 227.

(7) Barrer, R. M. *The Hydrothermal Chemistry of Zeolites*; Academic Press: London, 1982.

(8) Lok, B. M.; Carman, T. R.; Messina, C. A. *Zeolites* 1983, 3, 282.

(9) Deverell, C. In *Progress in NMR Spectroscopy*; Emsley, J. W., Feeney, J., Sutcliffe, L. H., Eds.; Pergamon: Oxford, 1969; Vol. 4, p 235.